International Journal of Computing and Optimization
Vol. 3, 2016, no. 1, 93 - 104
HIKARI Ltd, www.m-hikari.com
http://dx.doi.org/10.12988/ijco.2016.6613

Numerical Simulation of Traffic Flow via Fluid Dynamics Approach

Erwin B. Setiawan, D. Tarwidi, and Rian F. Umbara

School of Computing, Telkom University
Jalan Telekomunikasi Terusan Buah Batu, Bandung 40257, Indonesia

Abstract

This article deals with traffic flow simulation in a single road via fluid dynamics approach. The Lighthill-Whitham-Richards (LWR) model is used to describe traffic flow in the road which is represented by density and average speed of vehicles. Numerical approximation of the LWR model formulated as scalar conservation laws is obtained by implementing finite volume method. Several test cases are presented to simulate propagation of rarefaction and shock wave which arise in traffic flow phenomena. It has been shown that numerical results in term of density confirm the exact solutions. Numerical simulations of congestion triggered by the existence of traffic light are also discussed. The simulation results show that through adjusting the red and green light period, we can control traffic flow in traffic light location.

Keywords: LWR model, traffic flow, finite volume method, simulation

1 Introduction

Traffic jam in big cities such as Jakarta, Bandung, and Surabaya has become intricate urban problem. The congestion can be induced by roads perforated, no traffic sign, indiscipline of drivers, over capacity of roads, emergence of illegal parking, and misapplication of sidewalks. In addition, disproportional of the traffic light cycle in a junction also serves as cause of the congestion.

Some government's plans to solve traffic problems are suggestion to use public transportation, making the rule even/odd plat numbers, building mass rapid transit and new roads, and raising parking tax. However, all of these solutions have not been optimally able to overcome the congestion.

A solution to solve the increasingly complex congestion is to build an intelligent transportation system (ITS) [1]. The system consists of many subsystems which are placed in every heavy traffic road. Each subsystem has sensors to collect traffic data such as average speed and number of vehicles that pass a certain point per unit time and send it to ITS center. These data will be collected in a server for the simulation process. The simulation results obtained should be able to adjust the cycle time of traffic lights in every road intersection, provide an alternative path to avoid congestion, and predict when and where congestion will occur. This work is an ongoing effort to build the integrated intelligent transportation system with dynamics traffic assignment.

Since the beginning of the twentieth century, the researchers have begun to think of a mathematical model that can describe the behavior of traffic in urban areas. There have been two models developed to describe traffic flow—i.e. microscopic or car-following model and macroscopic model. In microscopic model, the traffic flow is described by the behavior of each single vehicle in the road. The movement of each vehicle is represented by ordinary differential equation where the dynamical equation depends on velocity and position of the next vehicle [2, 3, 4]. However, the microscopic model becomes complicated when in a road has large the number of vehicles. In macroscopic model, the traffic flow is described by mimic the movement of vehicles with the motion of fluid [5, 6, 7]. Here, the traffic flow is represented by density and average speed of vehicles.

The macroscopic model was first introduced by Lighthill and Whitham [8] in 1955 and independently by Richards [9] in 1956. The mathematical model introduced by Lighthill-Whitham-Richards is formulated as a nonlinear partial differential equation derived by the conservation of vehicles in a single road and referred to as LWR model. Bretti et al. [10] are discussed two numerical approximations to solve LWR model—i.e. classical Godunov scheme which is based on finite volume discretization and discrete velocities scheme.

This article focuses on numerical simulation of traffic flow via fluid dynamics model for a single road with a traffic light. Mathematical formulation to describe density and average speed of vehicles is given by the LWR equation. We adopt finite volume method to obtain numerical results for such model. Further comprehensive review of finite volume method can be found in [11, 12, 13, 14]. We examine several test cases to asses convergence of finite volume method. Numerical simulation of traffic light with adjusting red-green period is also discussed.

2 Mathematical Formulation

We consider LWR model which is based on fluid dynamics approach to describe traffic flow in a single road. This model is formulated as scalar hyperbolic conservation laws and can be written as [8, 9]:

$$\begin{cases} \dfrac{\partial \rho}{\partial t} + \dfrac{\partial q}{\partial x} = 0, \\ \\ \rho(x, t = 0) = \rho_0(x), \end{cases} \tag{1}$$

where $\rho \in [0, \rho_{max}]$ is the density of vehicles at position x and time t, ρ_{max} is the maximum density of vehicles where vehicles are immobile, and $\rho_0(x)$ is the initial condition of LWR equation. Furthermore, q is the number of vehicles across a point per unit time which is also called vehicles flux. Here, we assume that vehicles flux is a function of density which is given by

$$q(\rho) = \rho\, v, \tag{2}$$

where v is the average speed of vehicles.

We assume that the vehicles will adjust the speed almost instantly depend on the surrounding traffic condition. In other words, a driver tends to be cautious in the high traffic density and rises the speed in the lower traffic density. As consequence, v is a function that depends on ρ. Thus, v may be formulated as

$$v(\rho) = \left(1 - \frac{\rho}{\rho_{max}}\right) v_{max}, \tag{3}$$

where v_{max} is maximum speed which occurs when ρ tends to zero.

To construct the solution of (1), we introduce Riemann problem which is an initial-value problem defined as

$$\rho_0(x) = \begin{cases} \rho_L, & \text{for } x \le x_0 \\ \rho_R, & \text{for } x > x_0, \end{cases} \tag{4}$$

where ρ_L and ρ_R are constant values and x_0 is the location of the initial discontinuity.

3 Computational Method

We consider the finite volume method for solving LWR model in (1) with initial condition is given by (4). At first, the computational domain with length l is divided into M subintervals by finite volume discretization. Thus, we have length of subinterval $\Delta x = l/M$. Suppose subscript $j + 1/2$ denotes interface between node j and $j+1$ and superscript $n+1/2$ denotes time average of time level between n and $n+1$. Let ΔV_j is the area inside $[x_{j-1/2}, x_{j+1/2}]$ which is referred to as control volume (Figure 1).

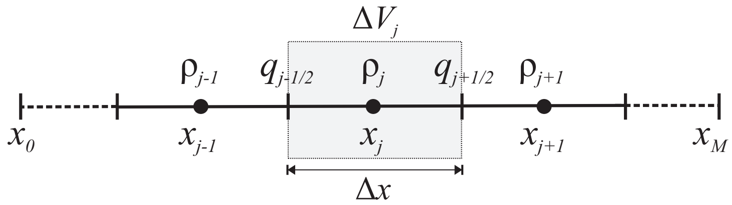

Figure 1: Finite volume discretization of $\rho(x,t)$ with control volume $\Delta V_j = [x_{j-1/2}, x_{j+1/2}]$.

Let ρ_j^n be average of $\rho(x,t)$ in control volume ΔV_j at time n. Now, vehicle flux that across interface $x_{j+1/2}$ can be written as

$$q_{j+1/2}(t) = q_{j+1/2}^{n+1/2} = q\left(\rho_{j+1/2}^{n+1/2}\right), \text{ for } t \in [t^n, t^{n+1}]. \tag{5}$$

By integrating (1) over control volume $[x_{j-1/2}, x_{j+1/2}]$ and time $[t^n, t^{n+1}]$, yields

$$\int_{x_{j-1/2}}^{x_{j+1/2}} \rho(x, t^{n+1})\, dx - \int_{x_{j-1/2}}^{x_{j+1/2}} \rho(x, t^n)\, dx = \int_{t^n}^{t^{n+1}} \left[q_{j-1/2}(t) - q_{j+1/2}(t)\right] dt. \tag{6}$$

By using Mean Value Theorem

$$\rho_j^n \approx \frac{1}{\Delta x} \int_{x_{j-1/2}}^{x_{j+1/2}} \rho(x, t^n)\, dx, \tag{7}$$

equation (6) can be written as

$$\rho_j^{n+1} = \rho_j^n + \frac{\Delta t}{\Delta x}\left(q_{j-1/2}^{n+1/2} - q_{j+1/2}^{n+1/2}\right), \tag{8}$$

where

$$q_{j+1/2}^{n+1/2} = \left(1 - \frac{\rho_{j+1/2}^{n+1/2}}{\rho_{max}}\right) v_{max}\, \rho_{j+1/2}^{n+1/2}. \tag{9}$$

Here, $\rho_{j+1/2}^{n+1/2}$ is the solution of the Riemann problem as defined in (4):

$$\rho(x, t^n) = \begin{cases} \rho_L = \rho_i^n, & \text{for } x \leq x_{i+1/2} \\ \rho_R = \rho_{i+1}^n, & \text{for } x > x_{i+1/2}. \end{cases} \tag{10}$$

The solution of the Riemann problem in (10) can be summarized in Table 1.

Table 1: Solution of the Riemann problem for the LWR equation [14].

Case	Structure of the solution	$\rho_{j+/2}^{n+1/2} =$
$\rho_j^n \geq \rho_j^n$ and $\rho_j^n < \rho_{max}/2$	Rarefaction wave heading to the right	ρ_j^n
$\rho_j^n \geq \rho_{max}/2$ and $\rho_{j+1}^n \leq \rho_{max}/2$	Rarefaction spreading to both left and right	$\frac{\rho_{max}}{2}$
$\rho_j^n \geq \rho_{j+1}^n$ and $\rho_{j+1}^n \geq \rho_{max}/2$	Rarefaction wave heading to the left	ρ_{j+1}^n
$\rho_j^n < \rho_{j+1}^n$ and $\rho_j^n + \rho_{j+1}^n \leq \rho_{max}$	Shock wave heading to the right	ρ_j^n
$\rho_j^n < \rho_{j+1}^n$ and $\rho_j^n + \rho_{j+1}^n > \rho_{max}$	Shock wave heading to the left	ρ_{j+1}^n

Since we use explicit time integral, the numerical scheme in (6) is conditionally stable. The stability of the numerical solution is guaranteed by

$$\Delta t \leq \min_{j=1,\ldots,M} \frac{\Delta x}{\left|1 - \frac{\rho_j^n}{\rho_{max}}\right| v_{max}\, \rho_j^n}. \tag{11}$$

4 Results and Discussion

In this section, we examine the convergence of finite volume method for solving LWR model with the initial condition is given by Riemann problem defined in (4). For this purpose, we need to calculate L^2 norm error which is given by

$$\|\rho(x,t) - \rho_{exact}(x,t)\|_{L^2} = \left(\int_0^l [\rho(x,t) - \rho_{exact}(x,t)]^2 \, dx \right)^{1/2}. \tag{12}$$

Here, equation (12) can be solved by the well-known Trapezoidal integration formula.

4.1 Test Case 1

The purpose of this test is to simulate propagation of shock wave triggered by the traffic light. Let we suppose the length of computational domain is 2000 m. At $x = 2000$ the traffic light is installed and initially the light is red. Further, we assume $v_{max} = 33$ m/s, $\rho_{max} = 0.25$ 1/m, initial vehicle density is 0.15 1/m, and vehicle density at the lef-hand and right-hand boundary are

0.15 1/m and 0.25 1/m respectively. Thus, we have the Riemann problem with $\rho_L = 0.15$, $\rho_R = 0.25$, and $x_0 = 2000$. The exact solution of this problem is given by

$$\rho(x,t) = \begin{cases} \rho_L, & \text{if } (x-x_0)/t < c_s \\ \rho_R, & \text{if } (x-x_0)/t > c_s, \end{cases}$$

where $c_S = [q(\rho_L) - q(\rho_R)]/(\rho_L - \rho_R)$.

Table 2: L^2 norm error and convergence rate for the Test Case 1.

M	$\|\rho_{num} - \rho_{exact}\|_{L^2}$	Ratio
20	0.506639	-
40	0.362436	0.483232
80	0.267273	0.439412
160	0.184095	0.537864
320	0.137368	0.422404

The density of vehicles for Test Case 1 using finite volume method against the exact solution is presented in Figure 2. From this figure, we can see that a shock wave induced by red light at $x = 2000$ m propagates from the right-hand boundary toward the computational domain. The L^2 norm error and convergence rate for Test Case 1 are listed in Table 2. This table shows that the errors become smaller as the cells are refined with the convergence rates are around 0.4 except at $M = 160$.

Table 3: L^2 norm error for the Test Case 2.

M	$\|\rho_{num} - \rho_{exact}\|_{L^2}$	Ratio
20	0.174981	-
40	0.135938	0.364249
80	0.101790	0.417353
160	0.072650	0.486561
320	0.048419	0.585390

4.2 Test Case 2

The second test case is conducted to simulate the propagation of rarefaction wave which is induced when the density of left-hand boundary is larger than other location inside computational domain. Here, we assume $v_{max} = 33$ m/s,

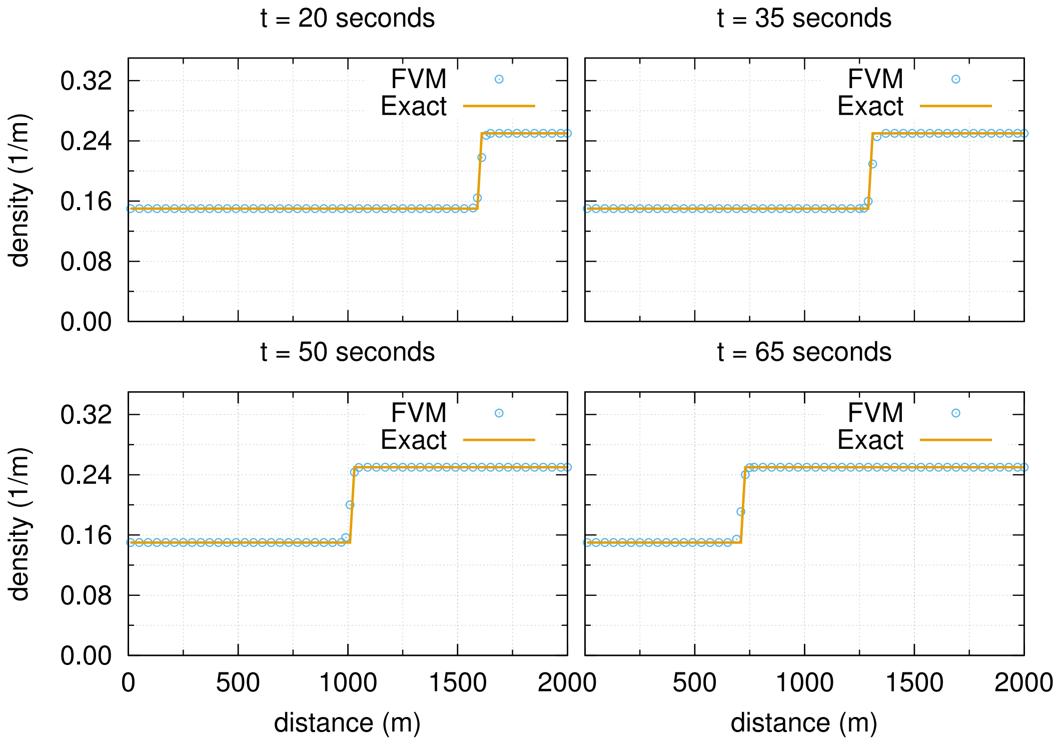

Figure 2: Finite volume method against exact solution of Test Case 1 for $t = 20$, $t = 35$, $t = 50$, and $t = 80$ seconds using $\Delta x = 20$ m and $\Delta t = 0.5$ seconds.

$\rho_{max} = 0.25$ 1/m, initial vehicle density is 0.02 1/m, and vehicle flux at the left-hand boundary is $q_b = 1.2$ 1/s. From equation (2) and (3), the left-hand boundary becomes

$$\rho(x = 0, t) = \frac{\rho_{max}}{2} - \frac{1}{2}\left(\rho_{max}^2 - 4\rho_{max} q_b / v_{max}\right)^{1/2}.$$

Then, we have the Riemann problem with $\rho_L = \rho(x = 0, t)$, $\rho_R = 0.02$, and $x_0 = 0$. The exact solution of this problem is given by

$$\rho(x,t) = \begin{cases} \rho_L, & \text{if } (x - x_0)/t < \lambda(\rho_L), \\ \frac{1}{2}\rho_{max}\left(1 - \dfrac{x - x_0}{v_{max}\, t}\right), & \text{if } \lambda(\rho_L) < (x - x_0)/t < \lambda(\rho_R), \\ \rho_R, & \text{if } (x - x_0)/t > \lambda(\rho_R), \end{cases}$$

where $\lambda(\rho) = (1 - 2\rho/\rho_{max})\, v_{max}$.

Figure 3 displays the density of vehicles for Test Case 2 using finite volume method against the exact solution. As can be seen from the figure, the a rarefaction wave appears since wave celerity at the boundary is smaller than

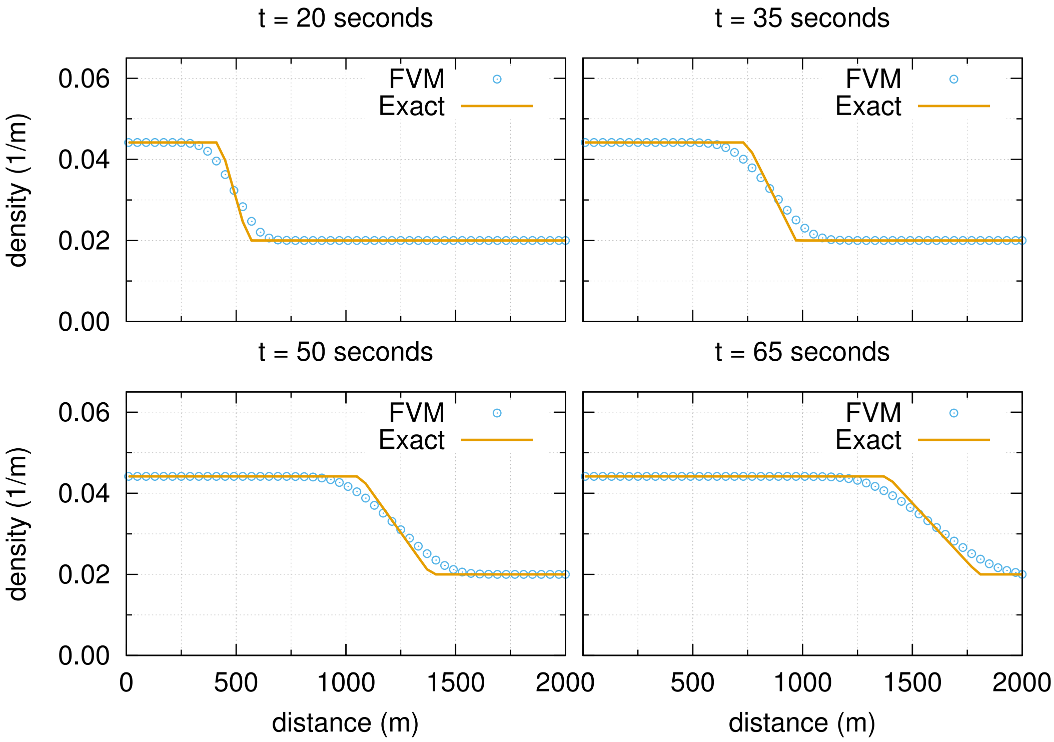

Figure 3: Finite volume method against exact solution of Test Case 2 for $t = 20$, $t = 35$, $t = 50$, and $t = 80$ seconds using $\Delta x = 20$ m and $\Delta t = 0.5$ seconds.

wave celerity inside the computational domain. The L^2 norm error and convergence rate for Test Case 2 are summarized in Table 3. As expected, the errors become smaller as the cells are refined with the convergence rates are increasing from 0.36 to 0.58.

4.3 Traffic Light Simulation

This simulation is presented to describe the density of the vehicles in a single road with a traffic light. Figure 4 illustrates cars queue in front of the traffic light. Here, the computational domain is $0 \leq x \leq 2000$ with traffic light

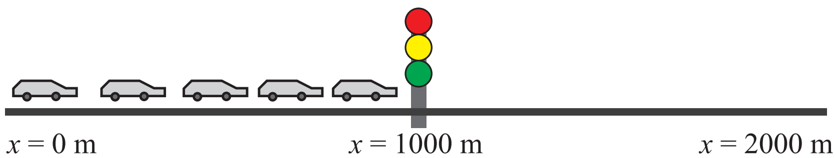

Figure 4: Illustration of vehicles queue at traffic light.

Table 4: Parameters for the traffic light simulation using LWR model.

Symbol	Parameter	Value
l	Length of computational domain	2000 m
ρ_L	Vehicles flux at left boundary	0.5 1/s
v_{max}	Maximum speed	33 m/s
v_R	Vehicles speed at right-hand boundary	non-reflective
ρ_0	Initial density	0.3 1/m
ρ_{max}	Maximum density	1 1/m
Δt	Time step	0.25 s
Δx	Cell size	10 m

position at $x = 1000$. We assume that at $t = 0$ the light is red. Suppose that Δt_g and Δt_r are the period of green and red light respectively. One of the causes of congestion at the traffic light is the management of red and green light period. In this simulation, we conduct three scenarios of green/red period. The first scenario, we set $\Delta t_r = 30$ seconds and $\Delta t_g = 5$ seconds. For the second and third scenario, we set green period is longer than first scenario—i.e. $\Delta t_g = 10$ seconds and $\Delta t_g = 20$ seconds respectively, while the red period is fixed. All parameters for this simulation are summarized in Table 4.

The density of vehicles for the three scenarios at $t = 32.5$, $t = 52.5$, $t = 65$, and $t = 80$ seconds is depicted in Figure 5. Since the first 30 seconds is red light, then the density of vehicles at $x = 1000$ becomes high and it generates shock wave propagating to the left hand direction. As consequence, it triggers the congestion in front of the traffic light with the length of cars queue is approximately 335 m. When the light turns green, we can see that the rarefaction wave is generated near $x = 1000$ m. At $t = 52.5$ seconds, for the first scenario ($\Delta t_g = 5$ s), the length of congestion is about 400 m and it reaches 635 m when $t = 65$ seconds. However, for the second scenario ($\Delta t_g = 10$ s), the length of congestion is about 255 m at $t = 52.5$ seconds and it attains 505 m when $t = 65$ seconds. Meanwhile, for the third scenario ($\Delta t_g = 20$ s) there is no significant congestion.

Figure 5 also reveals that after $t = 80$ seconds, for the first scenario, the length of congestion becomes longer and longer. In contrast, for the second and third scenario, the congestion can return unravel. Therefore, by this simple simulation we can see that through adjusting the values of Δt_r and Δt_g, we can control traffic flow in single road with traffic light.

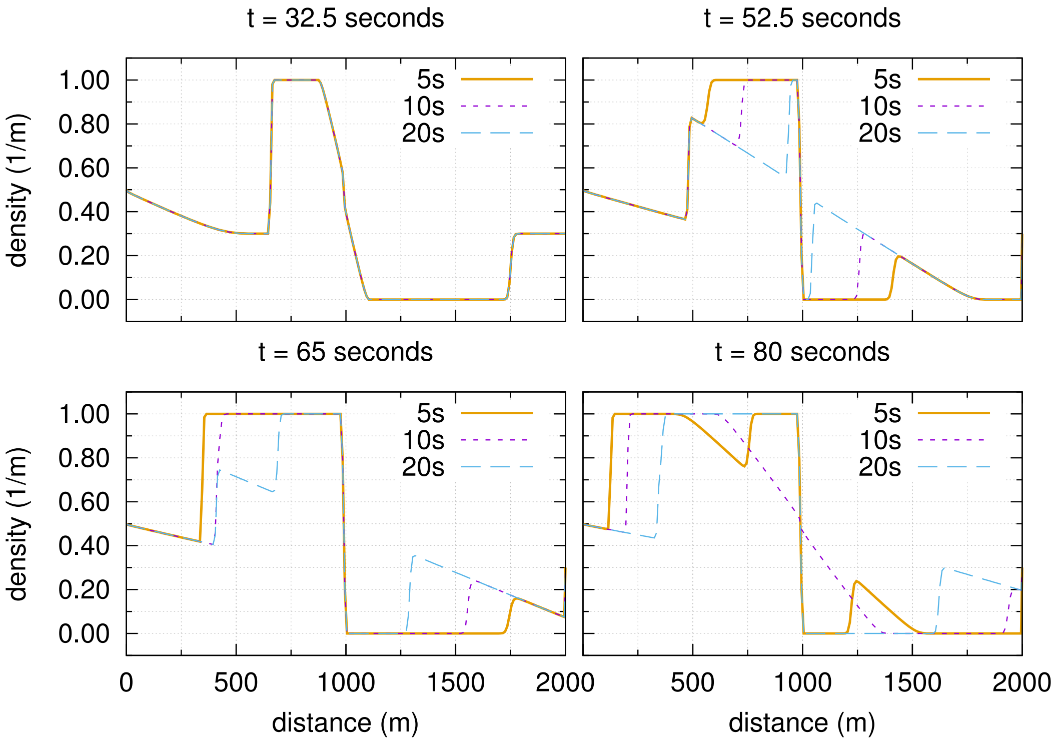

Figure 5: Density of vehicles for 30 seconds of red period and 5, 10, and 20 seconds of green period at $t = 32.5$, $t = 52.5$, $t = 65$, and $t = 80$ seconds.

5 Conclusion

Traffic flow in single road has been successfully simulated using finite volume method. The numerical results to describe propagation of rarefaction and shock wave which is induced by traffic light have been validated with the exact solution. It has been shown that finite volume method has good agreement with the exact solution. The numerical simulation of congestion triggered by traffic light has also been presented. It can be concluded that through adjusting the red and green light period, we can control traffic flow in traffic light location. Suggestion for the future research is to develop traffic flow simulation on road networks.

References

[1] M. Caramia, C. D'Apice, B. Piccoli, and A. Sgalambro, Fluidsim: A Car Traffic Simulation Prototype Based on Fluid Dynamic, *Algorithms,* **3** (2010), 294–310. http://dx.doi.org/10.3390/a3030294

[2] R.E. Chandler, R. Herman and E.W. Montroll, Traffic Dynamics: Studies in Car Following, *Operations Research,* **6** (1958), 165–184. http://dx.doi.org/10.1287/opre.6.2.165

[3] G.F. Newell, Nonlinear Effects in the Dynamics of Car Following, *Operations Research,* **9** (1961), 209–229. http://dx.doi.org/10.1287/opre.9.2.209

[4] M. Bando, K. Hasebe, A. Nakayama, A. Shibata, and Y. Sugiyama, Dynamical Model of Traffic Congestion and Numerical Simulation, *Phys. Rev. E,* **51** (1995), 1035–1042. http://dx.doi.org/10.1103/physreve.51.1035

[5] H.J. Payne, Models of Freeway Traffic and Control, *Math. Models Publ. Sys. Simul. Council Proc.,* **28** (1971), 51–61.

[6] A. Aw and M. Rascle, Resurrection of "Second Order" Models of Traffic Flow, *SIAM J. Appl. Math.,* **60** (2000), 916–938. http://dx.doi.org/10.1137/s0036139997332099

[7] H.M. Zhang, A Non-equilibrium Traffic Model Devoid of Gas-like Behavior, *Transportation Research Part B: Methodological,* **36** (2002), 275–290. http://dx.doi.org/10.1016/s0191-2615(00)00050-3

[8] M.J. Lighthill and G.B. Whitham, On Kinematic Waves. I: Flood Movement in Long Rivers, On Kinematic Waves. II: A Theory of Traffic Flow on Long Crowded Roads, *Proc. Royal Soc. A,* **229** (1955), 281–345. http://dx.doi.org/10.1098/rspa.1955.0088 http://dx.doi.org/10.1098/rspa.1955.0089

[9] P.I. Richards, Shock Waves on the Highway, *Operations Research,* **4** (1956), 42–51. http://dx.doi.org/10.1287/opre.4.1.42

[10] G. Bretti, R. Natalini and B. Picolli, A Fluid-Dynamic Traffic Model on Road Networks, *Archives of Computational Methods in Engineering,* **14** (2007), 139–172. http://dx.doi.org/10.1007/s11831-007-9004-8

[11] D. Tarwidi and S.R. Pudjaprasetya, Godunov method for Stefan problems with enthalpy formulations, *East Asian Journal of Applied Mathematics*, **3** (2013), 107–119. http://dx.doi.org/10.4208/eajam.030513.200513a

[12] R.J. Leveque, *Finite Volume Methods for Hyperbolic Problems,* Cambridge University Press, Cambridge, 2002. http://dx.doi.org/10.1017/cbo9780511791253

[13] E.F. Toro, *Riemann Solvers and Numerical Methods for Fluid Dynamics: A Practical Introduction,* Springer-Verlag, Berlin Heidelberg, 2009. http://dx.doi.org/10.1007/b79761

[14] V. Guinot, *Godunov-type Schemes: An Introduction for Engineers,* Elsevier Science B.V., Amsterdam, 2003.

Received: November 15, 2015; Published: June 24, 2016